This article can be cited as E. Sitompul and M. Y. Baihaqi, Quasi-Dynamic Walking Optimization of Humanoid Robot Using Genetic Algorithm, International Journal of Artificial Intelligence, vol. 20, no. 1, pp. 24-45, 2022.

Quasi-Dynamic Walking Optimization of Humanoid Robot Using Genetic Algorithm

Erwin Sitompul[1] and **Muhammad Yeza Baihaqi**[2]

[1]Study Program of Electrical Engineering, Faculty of Engineering,
President University, Cikarang (Indonesia);
Email: sitompul@president.ac.id

[2]Study Program of Electrical Engineering, Faculty of Engineering,
President University, Cikarang (Indonesia);
Email: muhammadyezab@gmail.com

ABSTRACT

Humanoid robot has been developed in design methods and functionality in recent years. In its application, a humanoid robot is required to interact with human, tools, or the environment. For a bipedal humanoid robot, efficient, precise, and stable walking is required, where the humanoid robot is expected to walk in a bigger step in a predetermined direction without falling. In this paper, the Genetic Algorithm (GA) is implemented to optimize the quasi-dynamic walking of a humanoid robot. The walking is optimized in terms of distance and precision while keep considering stability. For this purpose, a 10-DoF humanoid robot is designed and constructed to resemble a half-body of a human, from waist to feet. The humanoid robot is built of metal brackets where 10 servo motors are integrated for a coordinated movement. The walking gait of the humanoid robot for one complete walking cycle of one right step and one left step is divided into 8 walking phases. In each walking phase, the input to the 10 servo motors can be set whether with the same value as the previous phase or with a new value. The GA takes all possible new input values to the servo motors as the genes of an individual. At the population initialization, the first individual that can move the humanoid robot with adequate stability is found by using the forward kinematics method. Five individuals are derived from the first individual through mutation with the rate of 40-60 %. Thus, the GA starts with an initial population of these 6 individuals. A novel fitness function is introduced with positive weight on straightforward displacement and negative weight on deviation. This also emphasizes the merit of this research in the quantification of a robot's walking performance. The GA cycles include the uniform crossover with 25 % gene exchange probability and the mutation with the rate of 10 %. The GA is conducted for 4 cycles, where every individual is tested on the humanoid robot 10 times. In each test, the humanoid robot performs 3 complete walking cycles and the fitness score is assessed. The GA is successful to increase the fitness score of the population's best individual from 12.02 to 25.42. The walking distance is increased by 26.12 % from 25.33 cm to 31.94 cm, while the deviation angle is reduced by 57.65 % from 25.39° to 10.75°. Further application of the proposed method is to obtain the best individual for the robot to walk in a certain direction, which will possible by adjusting the fitness function. This is to be done with the support of sensor feedback and reverse kinematics in the robot's modeling.

Keywords: Humanoid robot, genetic algorithm, forward kinematics, quasi-dynamic walking.

Mathematics Subject Classification: 68W50, 68T20

Computing Classification System: Computing methodologies~Machine learning~Machine learning approaches~Bio-inspired approaches~Genetic algorithms

1. INTRODUCTION

A humanoid robot is a robot whose body shape resembles a human body. This kind of robot is created to collaborate with human or to replace human for finishing certain jobs (Behnke, 2008). Such kind of robot requires an ability to interact with human (Oztop *et al*., 2005). Humanoid robots have found applications in various fields (Asif *et al*., 2015; Riley and Atkeson, 2002). A humanoid robot capable of dancing is presented by Riley *et al*. (2000). A throw-and-catch humanoid robot can be found in the work of Kobey *et al*. (2012), which helps human to train to throw and catch a ball. The main challenges come from the integration of tasks such as walking, maintaining stability, interaction with humans, and variable environments (Hoffman *et al*., 2019). Some applications indeed require the humanoid robot to have stable and precise movement (Sandini *et al*, 2018). For example, in the case, that a humanoid robot is applied to conduct dangerous bomb disposal tasks or to play soccer. A precise movement to reach a bomb or a soccer ball is required.

Research in an effort to design a humanoid robot to play soccer was done by Afrisal *et al*. (2019). It is found that the robot has difficulty reaching the ball even though the ball is already located successfully. This is caused by the walking precision where the soccer robot is not only expected to have fast movement, but also precise walking. As the last example, a humanoid robot that is used to perform certain tasks in a nuclear facility also needs a stable and precise walking gait (Garcia *et al*., 2007).

Previous works to develop humanoid robot’s walking performance can be found in (Liu *et al*., 2017), where momentum compensation strategies were used to maintain the robot’s balance. Another humanoid robot research done by Mousavi *et al*. (2017) uses a model predictive control to stabilize the standing pose of the humanoid robot. Hashimoto and Takanashi (2015) developed a half-body biped humanoid robot and a human-carrying biped vehicle. Khan *et al* (2008) simulated the balancing of a four-degree-of-freedom (4-DoF) humanoid robot by using a PID control with the same approach as balancing a pendulum, as the robot performs the walking movement. In conclusion, many research efforts focus on using an algorithmic approach to develop the standing stabilization and walking stabilization of humanoid robots. Emphasis on walking precision and step size are the new aspects that will be considered in this research.

An optimization method needs to be applied to optimize the walking performance of a humanoid robot. The heuristic algorithm approach provides a number of choices. The Harmony Search Algorithm was successfully implemented to improve the flexibility of a traffic light controller in handling variable traffic density (Sitompul and Bunawan, 2011). Furthermore, a method to integrate the Genetic Algorithm in the generation of the fuzzy logic controller with minimum knowledge of the system is reported by Sitompul and Bukhori (2013). Dragos *et al*. (2021) presented the application of Grey Wolf Optimizer to tune the parameters of proportional-integral-fuzzy controllers. Multi-parametric quadratic programming is coping with nonlinear processes, in finding the best parameters of fuzzy controllers (Preitl *et al*., 2006). Furthermore, a hybrid algorithm is found to be able to reduce the construction time of wasp nests (Zapata *et al*., 2020).

Based on the problem stated above, the author intends to utilize the Genetic Algorithm (GA), given the scope of its certain mechanics (Manikas *et al*., 2007; Šegota *et al*., 2020). The humanoid robot used in this research is a 10-DoF humanoid robot, self-designed and self-constructed for the purpose of the research. The robot's walking gait is categorized into quasi-dynamic, where the whole surface of the feet will touch the surface while stepping (He *et al*., 2019). A series of tests will be conducted directly on the robot, instead of performing the simulation on a virtual model (Maiorino and Muscolo, 2020). The first individual, the base walking gait of the humanoid robot, is to be generated through the forward kinematics method. The initial population will be derived from the first individual. Afterward, the GA cycles are carried out by utilizing a fitness function that promotes forward displacement and penalizes deviation. This research is expected to be the basis for further research on the humanoid robot field, to develop a more precise walking gait and longer walking step, by using an algorithmic approach.

2. METHODOLOGY

2.1. Assembly of the 10-DoF Humanoid Robot

In this research, a 10-DoF humanoid robot is designed and constructed. Each freedom of movement is powered by one MG996R servo motor, with a maximum stall torque of 11 kg/cm. The humanoid robot is equipped with an Arduino Uno R3 microcontroller to run the movement program.

The chassis of the humanoid robot is built of metal brackets with various shapes. The brackets are fastened to each other by bolts, as they are assembled to form the feet, the legs, the thighs, and the waist. The servo motors are placed accordingly at the joints of both body sides: 2 for each ankle, 1 for each knee, and 2 for each hip. Figure 1 shows the humanoid robot after the construction is completed.

The wiring from the microcontroller to all the servo motors, as the mean of control signal transmission, can be seen clearly. Two external 9V/2A power sources are used to provide electrical power to the servo motors, while one USB cable is connected to power up the microcontroller. The block diagram in Figure 2 shows the interconnection of the microcontroller, the servo motors, and the power sources. The blue line represents the flow of information or data, while the red line indicates the flow of electrical power.

Figure 1. The 10-DoF humanoid robot

The inputs to each servo motor are given in degree number, from 0 to 180. Later, this degree number will be converted to a corresponding voltage to be applied to the servo motors. If a degree number is given, then the servo motor will rotate to the desired position with the speed proportional to the difference between the current position and the desired position. Once the desired position is reached, the same number should be kept given as the input to the servo motor, so that it can maintain the position.

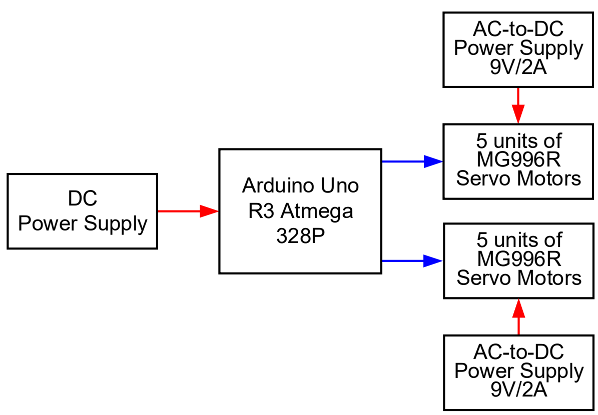

Figure 2. Block diagram of the humanoid robot

2.2. Implementation of the Genetic Algorithm

The GA is an optimization method based on the idea of natural selection. It can be used to solve constrained or unconstrained problems. Possible solutions are represented as individuals that constitute a population. Every individual has a set of characteristic parameters referred to as genes. In every generation, after a successful parent selection, the population produces a set of offspring through the process of crossover and mutation (Haldurai *et al.*, 2016). A fitness function is used to measure the suitability of the individuals to become the solution to the optimization problem (Chande and Sinha, 2008). By simulating the natural process of selection, only individuals with the best fitness score can survive and go to the next generation. Hereby the size of the population is maintained to be the same. The GA applied in this paper is as depicted by the flowchart in Figure 3.

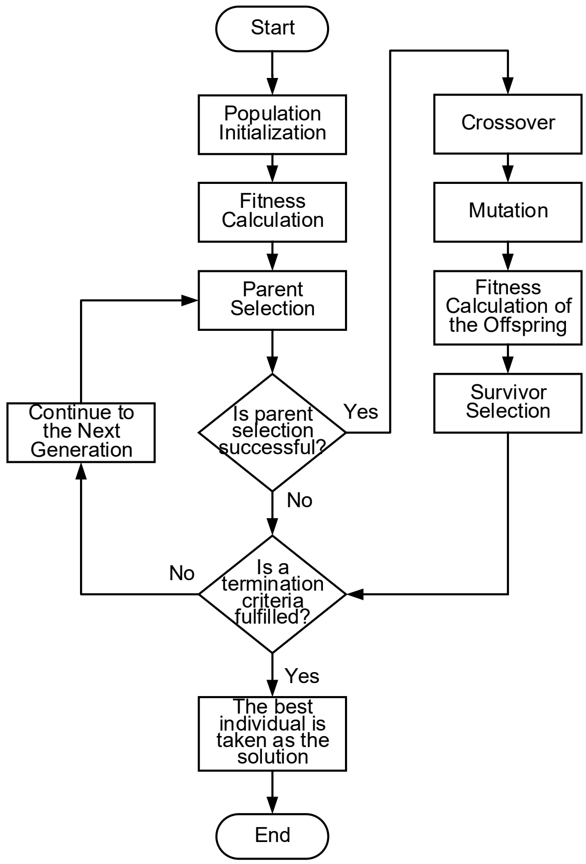

Figure 3. The applied Genetic Algorithm

In this stage, the GA is used to optimize the walking performance of the humanoid robot, in terms of high straightforward displacement and low deviation. First, a walking algorithm will be defined. A complete cycle of walking, or a walking gait, is divided into 8 walking phases, where the first 4 phases are to do the right step, and the last 4 phases are to do the left step. The complexity of finding a proper two-leg walking movement for the humanoid robot is high in terms of increased stability consideration. A comparison can be made with the design of a four-leg pet robot as discussed by Lumoindong and Sitompul (2021), where a gait with 2 or 4 phases is adequate.

In every walking phase, there are 10 values to be sent to the 10 servo motors. The walking algorithm is applied by entering these values into the inputs of the servo motors. By applying the values from walking phase 1 until walking phase 8, a complete walking algorithm is obtained. Figure 4 shows the arrangement of the 10 servo motors at the humanoid robot.

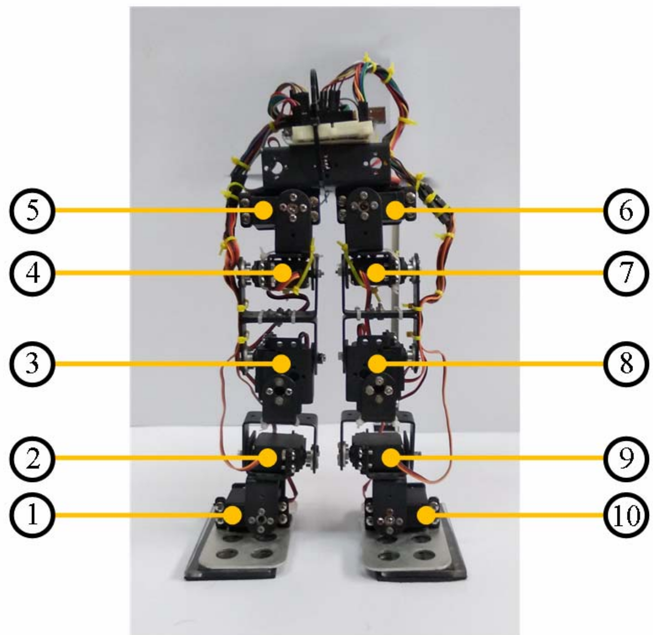

Figure 4. The installation location of the servo motors

The values to be given to the servo motors are integers from 0 to 180, representing the position of each servo motor in degree. To start the GA process, a first individual with a base walking gait needs to be found. This is done by a series of trial-and-error forward kinematics. In this finding process, a sequence of servo motors' change can be observed to make the humanoid robot walk a full step cycle (one step of the right leg followed by one step of the left leg) with acceptable speed and stability. Apparently, not all servo motors should change their positions in each walking phase. There are occasions where the servo motors only need to maintain the position from the previous phase.

For better illustration, Figure 5 shows the input values of the 10 servo motors at the first walking phase. If a servo motor obtains a new position at this first walking phase, then its value is labeled as X. If the position of a servo motor is the same as the one at the previous phase, then this value is labeled as NC (no change).

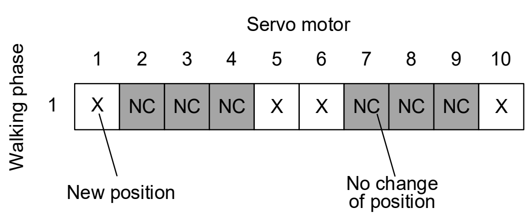

Figure 5. The position of the servo motors at the first walking phase

Figure 6 shows the complete walking gait of the humanoid robot, consisting of all 8 walking phases. Out of 80 possible servo positions, 38 are new positions while 42 are NCs. In the GA process, such a complete walking gait will be referred to as an individual. Thus, each individual has 38 genes whose values are to be optimized. As many as 6 individuals will make a population, as can be seen in Figure 7.

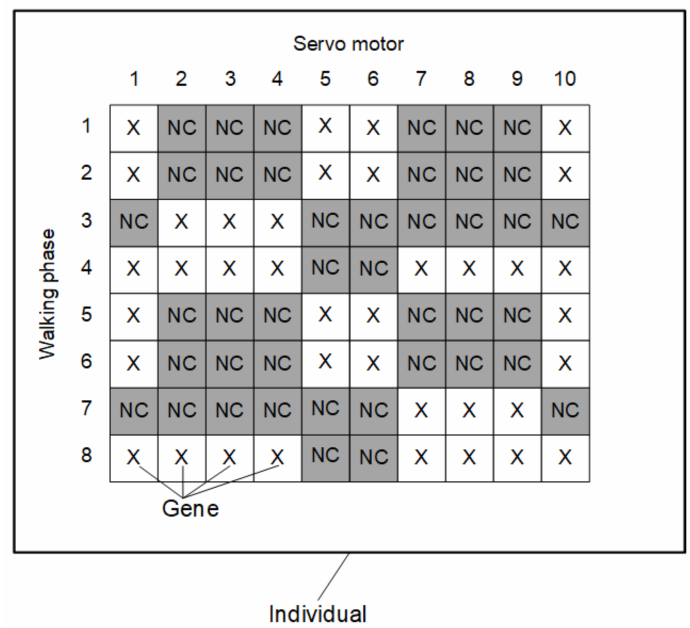

Figure 6. One individual as one complete walking gait of the humanoid robot

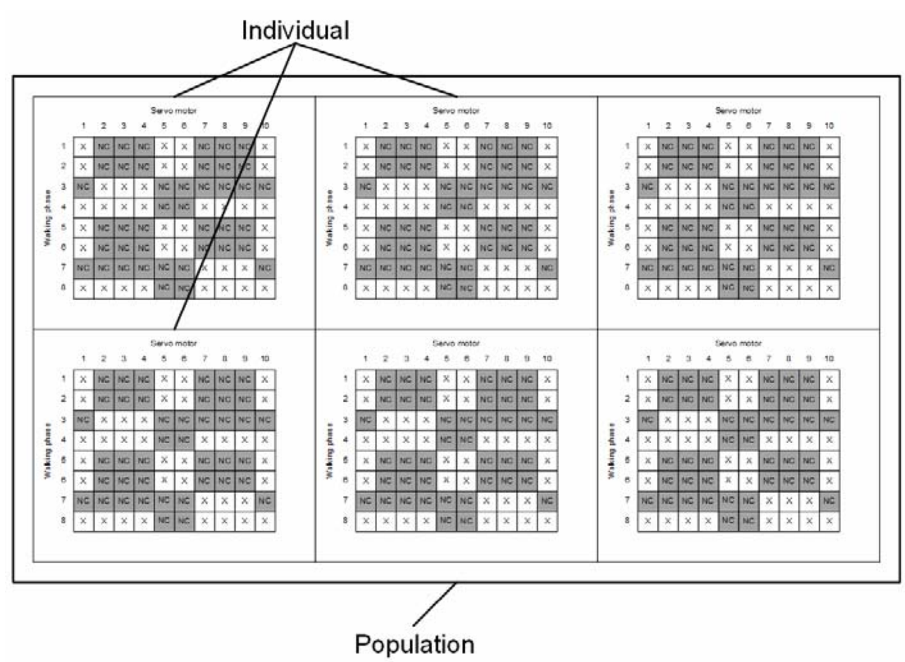

Figure 7. One population with 6 individuals

The parts of the GA process, as shown in Figure 3, will now be discussed in detail. This is to be done by considering the structure of the genes and the individuals already chosen at this point.

1. *Population Initialization*. The number of individuals in the population is chosen to be 6. There are 15 possible parent pairs if 2 individuals are picked out of 6. This provides adequate search space while keeping the population size manageable for the humanoid robot as a physical system. After the first individual is obtained, 5 further individuals are derived from it. This is done by randomly adding ± 1, ± 2, or ± 3, to 40-60 % of the first individual's 38 genes.

2. *Fitness Calculation and Parent Selection*. The fitness calculation is done by using a fitness function as given by the equation of

$$\text{Fitness Score} = F - R\,, \tag{1}$$

where *F* denotes the forward displacement and *R* is the deviation, to the left or the right, with the reference of the direction of straightforward displacement. The aspired walking optimization of the humanoid robot is attached to the fitness score as given in Equation (1). Hereby, an optimization problem may consist of minimizing a real function in the form of a cost function or error function. On the other hand, an optimization problem can also be defined as how to maximize a real function, which is the case in the applied Genetic Algorithm in this research. In this relation, maximizing the fitness score function is equivalent to optimizing the walking performance of the humanoid robot, with the setting of the servo motors as the free variables.

Figure 8 shows the forward displacement vector **F** and the deviation vector **R**. vectors, where the displacement vector **D** is given by **D** = **F** + **R**. Henceforth, *F* is the magnitude of the vector **F**, while *R* is the magnitude of the vector **R**.

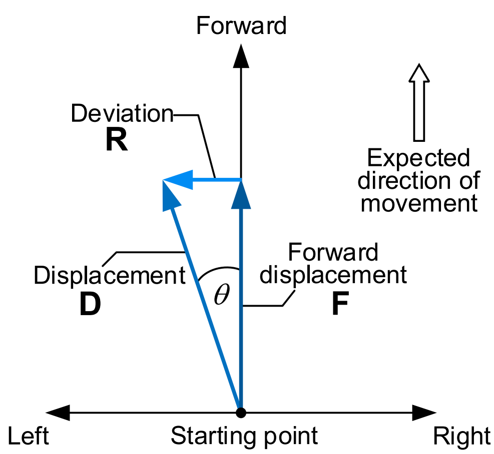

Figure 8. The components of the fitness function, **F** and **R**

To increase the forward displacement *F* and reduce the deviation *R*, the humanoid robot must walk a great displacement *D* while keeping the deviation angle *θ* small. Due to the minus term of the deviation, a large displacement but with a large deviation will not result in a higher fitness score. Thus, the fitness function endorses a movement with greater distance while simultaneously give merit to accuracy.

A further illustration is given in Figure 9. The displacement vector $\mathbf{D}_2$ is slightly greater than the displacement vector $\mathbf{D}_1$. However, the deviation vector $\mathbf{R}_2$ is significantly greater than the deviation vector $\mathbf{R}_1$. This causes the fitness score of the first movement ($F_1 - R_1$, a scalar value) to be greater than the one of the second ($F_2 - R_2$, also a scalar value), which is apparently negative.

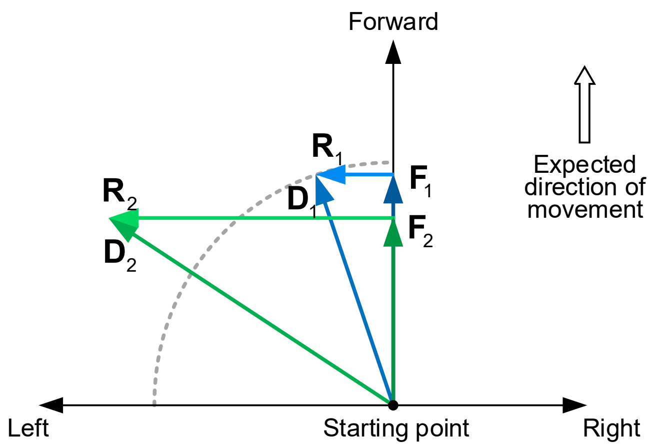

Figure 9. A great displacement with low accuracy results in a low fitness score

The parent selection is preceded by the selection of parent candidates. For this purpose, the tournament method is used. The scheme is described in Figure 10. Out of 6 population members, 3 are randomly chosen to be the tournament participants. Out of these 3 participants, a tournament winner is chosen based on the highest fitness score. A tournament winner automatically becomes a parent candidate (Jebari *et al*., 2013). In each generation, 3 tournaments are conducted, where it is possible to get the same winner at multiple tournaments. Thus, the tournaments can produce 1, 2, or 3 parent candidates.

If there is only 1 parent candidate, then the generation ends without any crossover and mutation. If there are 2 parent candidates, then both individuals are directly chosen as parents. Finally, if there are 3 parent candidates, then 2 parents will be chosen by using a weighted probability, based on the candidates' fitness scores.

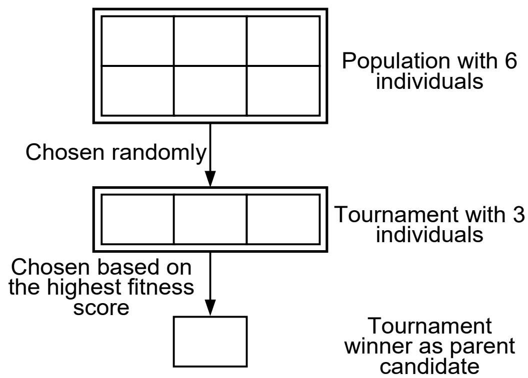

Figure 10. Scheme of a tournament to obtain a parent candidate

The weighted probability for each of the 3 parent candidates is calculated by using the linear ordinal-based rank (Pandey, 2016; Jebari *et al*., 2013):

$$P(K) = \frac{2(N-K)}{N(N+1)} \tag{2}$$

where P denotes the probability of the candidate with the relative rank K of N parent candidates. K takes the value 0 for the candidate with the highest fitness score and N–1 for the lowest. Hence, with $N = 3$, $P(0) = 6/12$, $P(1) = 4/12$, and $P(2) = 2/12$.

3. *Crossover*. In this research, if the parent selection is successful, then the crossover will always occur. The crossover becomes instrumental to obtain offspring, expected to be significantly new individuals. This is required to reach the optimum solution as quickly as possible. The uniform crossover is chosen to be implemented, which provides a wider variety of resulted offspring compared to other crossover methods such as one-point crossover and multi-point crossover (Mallawaarachchi, 2017; Soon *et al*., 2013; Sastry and Goldberg, 2003). The exchanged genes (or crossover rate) will be randomly chosen with a probability of 25 %.

4. *Mutation*. The mutation immediately occurs to the two offspring (new individuals) which are produced by the crossover. Thus, the mutation occurs with 100% probability in case a cycle generates new individuals. This value is chosen to maximize the search for the optimum solution within a limited number of cycles. The mutation rate is chosen to be 10 %. Thus, 10 % of the genes of the two offspring will be randomly added by ± 1, ± 2, or ± 3. Prior experiments with the humanoid robot show that this 10% provides a good balance between performance and improvement.

5. *Termination Point*. Two conditions are selected for the termination, where the GA will be stopped and the current best individual will be taken as the solution. The first termination condition is if the improvement of the best fitness score is less than 2 % in two consecutive cycles. The second termination condition is if the number of generations reaches 4. The number of walking tests that must be conducted on the humanoid robot for each individual limits this number of generations. This is due to the consideration regarding the mechanical exertion experienced by the humanoid robot.

Pseudocode that summarizes the Genetic Algorithm specifically used in this research is presented in Figure 11. Furthermore, the code of programs that can be used to generate the initial population and perform the crossover operation and the mutation operation program is accessible via http://bit.ly/GA_HR.

The GA has several random parameters such as the crossover rate, mutation rate, and the changes of gene values. By having these random parameters, the variability of the offspring is high and the available search space for the best solution is large. However, there is no guarantee that the best solution can be found after a certain number of cycles. If the algorithm fails to find the expected solution, it is to be repeated until the solution is found. The system to be optimized, the 10-DoF humanoid robot, is highly non-linear and there is always a possibility to be trapped in local minima. However, as the variability of the offspring is high and the search space is large, it is legitimate to expect an increasing fitness score by the flexibility of the termination conditions.

```
Data : First individual
Result : Final population with best individual
Generate the initial population from the first individual
Apply all individuals of the initial population to the humanoid
robot
Calculate the fitness score for each individual in the initial
population by using Equation (1)
while none of the two termination conditions is met do
    Select two parents in the population, using Equation (2)
    where applicable
    if two parents can be selected then
        Perform the crossover operation
        Perform the mutation of offspring
        Apply the offspring to the humanoid robot
        Calculate the fitness score for each offspring
        Perform the survivor selection
        Replace old population with new population
    end if
end while
return the final population with best individual
```

Figure 11. The pseudocode of the Genetic Algorithm

3. RESULTS AND DISCUSSIONS

3.1. Experiment Set-Up

During the experiment, the humanoid robot performs the walking movement on a flat surface made of plywood. The walkway is presented in Figure 12. The surface gives a perfect grip for the robot's feet and guarantees a uniform condition for all walking tests. The size of the surface is 50 cm × 50 cm.

The numerical values of every individual are applied to the humanoid robot as it performed 10 walking tests in a row. In each test, 6 steps are conducted, alternatingly 3 right steps and 3 left steps.

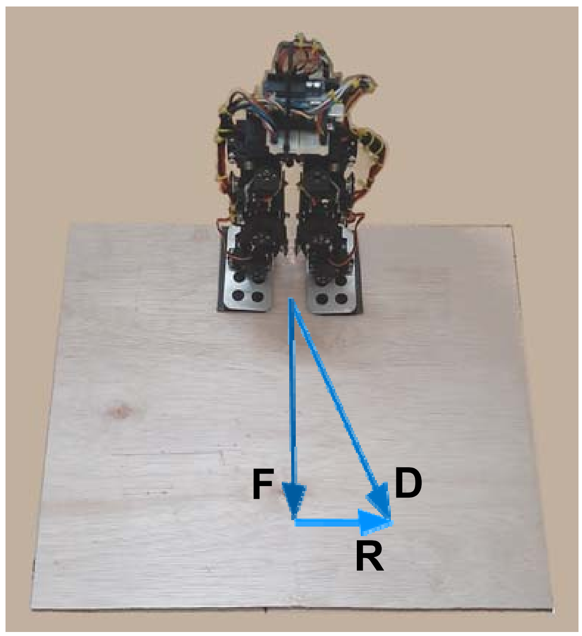

Figure 12. The walkway of the humanoid robot

3.2. Generating the Population

The first individual or the base walking gait is shown in Figure 13. Referring back, this figure is actually the application of the individual, whose original structure is shown in Figure 6. All empty gene compartments (earlier filled with X) are now filled with numbers between 0 and 180, which is obtained from trial-and-error forward kinematics.

The humanoid robot always starts from the standing position of [158, 75, 43, 40, 42, 30, 80, 143, 65, 105]. Then, in a continuous cycle, phase 1 until phase 8 are fed to the humanoid robot, as it keeps stepping forward. In each phase, the servo motors are held at any given position for 500 milliseconds. Thus, it takes 4 seconds to complete the 8 walking phases.

Walking phase \ Servo motor	1	2	3	4	5	6	7	8	9	10
1	163	NC	NC	NC	40	35	NC	NC	NC	111
2	172	NC	NC	NC	48	40	NC	NC	NC	116
3	NC	78	54	62	NC	NC	NC	NC	NC	NC
4	160	85	43	43	NC	NC	40	126	80	135
5	169	NC	NC	NC	45	35	NC	NC	NC	90
6	144	NC	NC	NC	30	20	NC	NC	NC	85
7	NC	NC	NC	NC	NC	NC	70	140	70	NC
8	158	65	62	70	NC	NC	80	145	65	100

Figure 13. The first individual (base walking gait)

Afterward, five further individuals are derived from the first individual. This is done by the method already explained as *Population Initialization* in the previous section. At the end of this stage, the whole population with 6 individuals, as depicted in Figure 7, is established. The humanoid robot is given the servo motor setting as represented by each individual through the microcontroller. Then, the robot is commanded to walk 10 consecutive times and the data of forward displacement and the deviation are measured and averaged. Next, the *Fitness Calculation* for the 6 individuals is conducted. Based on the measurement data, the fitness score can be calculated by using Equation (1).

The detailed performance of the initial population is shown in Table 1. The number of fall downs, the mean forward displacement (F), the mean deviation (R), and the mean fitness score ($F–R$) are presented. The calculation of the fitness score is as governed by Equation (1).

The number of fall downs is always zero. This implies that the initial population provides a stable walking for the humanoid robot. The unit for the forward displacement, the deviation, and the fitness score is centimeter.

Table 1: Walking performance of the initial population.

Item	*Individual*					
	1st	2nd	3rd	4th	5th	6th
Fall downs	0	0	0	0	0	0
Mean forward displacement (F)	27.54	24.11	22.88	21.02	21.65	28.19
Mean deviation (R)	15.86	19.83	10.86	25.42	24.20	17.68
Mean fitness score ($F–R$)	11.68	4.28	12.02	−3.40	−2.55	10.51

The humanoid robot always creates a left-deviation for all individuals of the initial population. This kind of problem was also found in (Allgeuer and Behnke, 2018). The reason can be the uneven effectiveness between the left leg and the right leg, where the latter is more effective. Moreover, this can be caused by the non-uniformity of the servo motors. The GA is expected to cope with this problem and give adequate compensation so that the forward displacement can be increased and the deviation can be decreased (Hwang *et al.*, 2015).

3.3. Genetic Algorithm Cycles

1. *First Cycle*

The GA cycle continues further according to the algorithm as shown in Figure 3 until a certain termination condition is fulfilled. The *Parent Selection* among the population ensues through the tournament method. For this first cycle, the tournaments result in two different winners, as shown in Table 2. Both the first and the second individuals are chosen as parents. Two offspring are generated through the *Crossover* and the *Mutation*, which are the seventh and the eighth individuals. Their performance is shown in Table 3.

Table 2: Tournament result of the first cycle.

Tournament	*Participating individuals*			*Winner*
1	1st	6th	2nd	1st
2	2nd	1st	5th	1st
3	2nd	4th	5th	2nd

Table 3: Walking performance of the 7th and the 8th individuals.

Item	*Individual*	
	7th	8th
Fall downs	0	0
Mean forward displacement (*F*)	28.84	25.72
Mean deviation (*R*)	13.49	11.17
Mean fitness score (*F*–*R*)	15.35	14.55

Based on the mean fitness score, both offspring are selected to become the new members of the population. The population at the end of the first cycle is shown in Table 4. The best fitness score is increased from 12.02 to 15.35, which corresponds to 27.70%. No termination condition is fulfilled and the algorithms proceed to the second cycle.

Table 4: The population at the end of the first cycle.

Rank	*Individual*	*Fitness score*
1	7^{th}	15.35
2	8^{th}	14.55
3	3^{rd}	12.02
4	1^{st}	11.68
5	6^{th}	10.51
6	2^{nd}	4.28

2. *Second Cycle*

In this cycle, all 3 tournaments result in the same winner, as shown in Table 5. The fittest 7^{th} individual is always chosen to be a tournament participant and wins. Thus, the second cycle does not produce offspring and the population at the end of the second cycle is unchanged. This also means that the best fitness score does not improve, making the count of the first termination condition equals 1. Since the count is not equal to 2 and the number of cycles is still below 4, the algorithm continues to the third cycle.

Table 5: Tournament result of the second cycle.

Tournament	*Participating individuals*			*Winner*
1	2^{nd}	6^{th}	7^{th}	7^{th}
2	2^{nd}	1^{st}	7^{th}	7^{th}
3	7^{th}	5^{th}	2^{nd}	7^{th}

3. *Third Cycle*

In this cycle, three different individuals become the winner of the three tournaments, as summarized in Table 6. All three become the parent candidates. In order of fitness scores, they are the 7^{th}, the 3^{rd}, and the 1^{st} individual.

Table 6: Tournament result of the third cycle.

Tournament	*Participating individuals*			*Winner*
1	2^{nd}	1^{st}	3^{rd}	3^{rd}
2	2^{nd}	6^{th}	7^{th}	7^{th}
3	6^{th}	1^{st}	2^{nd}	1^{st}

The weighted probability of the parent candidates is obtained by using Equation (2). The result is visualized in Figure 14. After the roulette disk rotation process, the 3^{rd} and the 1^{st} individuals are selected to become the parents. The resulting offspring are presented in Table 7.

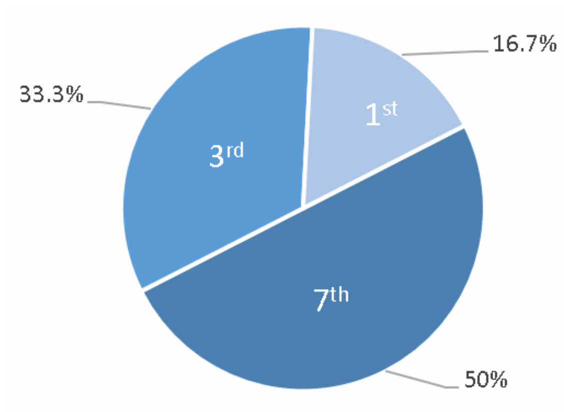

Figure 14. The probability of the parent candidates in the third cycle

Table 7: Walking performance of the 9th and 10th individuals.

Item	*Individual*	
	9th	10th
Fall downs	0	0
Mean forward displacement (*F*)	30.82	31.38
Mean deviation (*R*)	6.75	5.96
Mean fitness score (*F*–*R*)	24.07	25.42

Again, both offspring are qualified to become the members of the population. Their fitness scores rank the top two. The 9th and the 10th individuals deliver significant improvements compared to the former best 7th individual. The population at the end of the third cycle is presented in Table 8. The best fitness score is improved by 65.60%, from 15.35 of the 3rd individual to 25.42 of the 10th individual. This improvement resets the count of the first termination condition back to 0. The algorithm proceeds to the fourth cycle since no termination condition is met.

Table 8: Population at the end of the third cycle.

Rank	*Individual*	*Fitness score*
1	10th	25.42
2	9th	24.07
3	7th	15.35
4	8th	14.55
5	3rd	12.02
6	1st	11.68

4. *Fourth Cycle*

In the fourth cycle, the tournaments result in 2 different winners. Both are automatically selected as parents. The tournament summary can be seen in Table 9. The resulting offspring and their extremely different performance are presented in Table 10.

Table 9: Tournament result of the fourth cycle.

Tournament	*Participating individuals*			*Winner*
1	9th	3rd	7th	9th
2	7th	1st	3rd	7th
3	7th	9th	8th	9th

Table 10: Walking performance of the 11th and 12th individuals.

Item	*Individual*	
	11th	12th
Fall downs	0	0
Mean forward displacement (*F*)	21.19	29.60
Mean deviation (*R*)	21.80	6.62
Mean fitness score (*F*–*R*)	–0.61	22.98

The 11th individual yields a negative fitness of –0.61 and cannot better any current members of the population. On the other hand, the 12th individual produces a good fitness of 22.98, which occupies the third rank in the new population. The population at the end of the fourth cycle is shown in Table 11.

After the completion of the fourth cycle, the *Termination Point* is reached. Hereby, the second termination condition is fulfilled. Thus, the algorithms stop here.

Table 11: Population at the end of the fourth cycle.

`Rank	*Individual*	*Fitness score*
1	10th	25.42
2	9th	24.07
3	12th	22.98
4	7th	15.35
5	8th	14.55
6	3rd	12.02

5. *Assessment of the Overall GA Process*

The applied GA improves the walking performance of the humanoid robot. Figure 15 shows the course of the best fitness score of the population, from the initial population at the zeroth cycle until the final population after the fourth cycle.

The 3rd individual is the best individual of the initial population with a mean forward displacement of 22.88 cm and a mean deviation of 10.86 cm. This corresponds to the fitness score of 12.02. After four cycles of GA, the 10th individual becomes the best individual with a mean forward displacement of 31.38 cm and a mean deviation of 5.96 cm. This corresponds to the fitness score of 25.42. It can be observed that the 10th individual simultaneously delivers more forward displacement and less deviation.

Comparing both individuals further, the displacement (walking distance) is increased by 26.12 % from 25.33 to 31.94, while the deviation angle is reduced by 57.65 % from 25.39° to 10.75°.

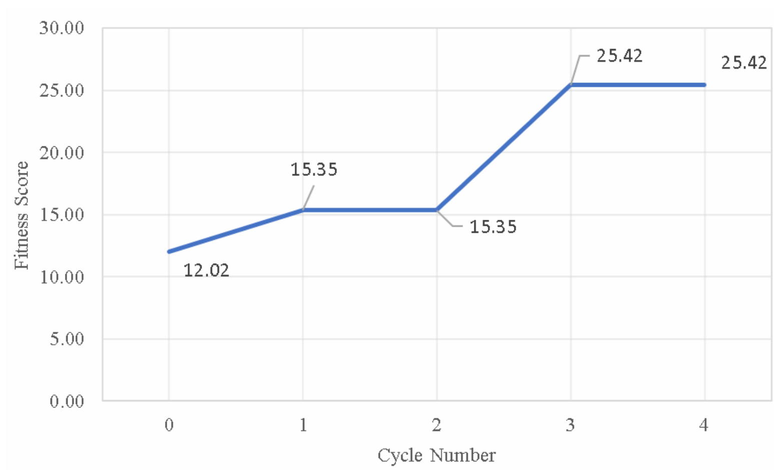

Figure 15. The highest fitness score in every cycle

Figure 16 presents the direct comparison between the individuals of the initial population and the final population, lined up based on the fitness scores, from the highest until the lowest. As mentioned previously, the fitness score is obtained from the mean forward displacement (*F*) subtracted by the mean deviation (*R*). The increase of the fitness score is the combination of the increase of *F* and the decrease of *R*. It also reflects the increased ability of the humanoid robot to walk straightway forward.

Only one individual from the initial population, the 3rd individual, survived the cycles and still becomes a member of the final population. All other new members of the population perform even better than the 3rd individual, which is now placed in the sixth position.

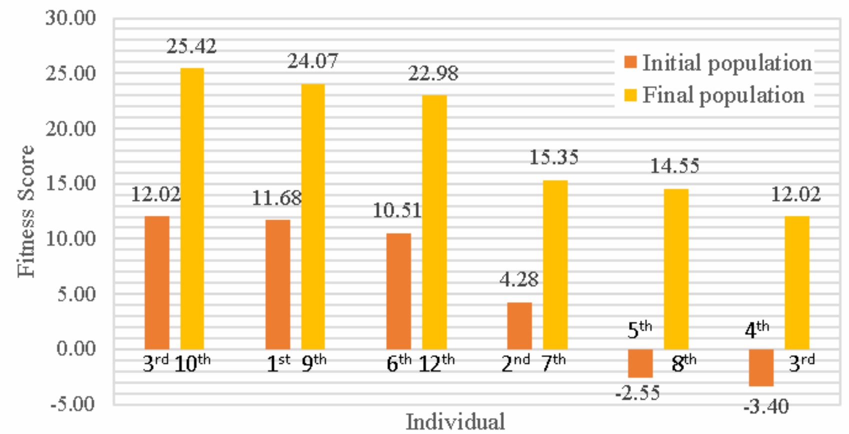

Figure 16. Fitness score comparison of the initial population and the final population

Figure 17 recaps the difference of gene values between the best individual (the 10th) and the first individual. The changes, indicated in green, can be found in 13 out of 38 genes. Figure 18 recaps the difference of gene values between the worst individual (the 4th) and the first individual. The changes, indicated in blue, can be found in 20 out of 38 genes. The difference, though seems to be small, summed up to be significant. It is proved from the experiments that the small changes make a big difference in the walking performance of the humanoid robot.

Servo motor

Walking phase	1	2	3	4	5	6	7	8	9	10
1	0	NC	NC	NC	0	+1	NC	NC	NC	0
2	0	NC	NC	NC	+1	−1	NC	NC	NC	0
3	NC	+1	0	+1	NC	NC	NC	NC	NC	NC
4	0	0	0	0	NC	NC	0	0	0	0
5	−3	NC	NC	NC	0	−2	NC	NC	NC	0
6	0	NC	NC	NC	0	+2	NC	NC	NC	+2
7	NC	NC	NC	NC	NC	NC	+1	0	+1	NC
8	0	0	−1	+1	NC	NC	0	0	0	0

Figure 17. The difference of gene values between the best individual (the 10th) and the first individual

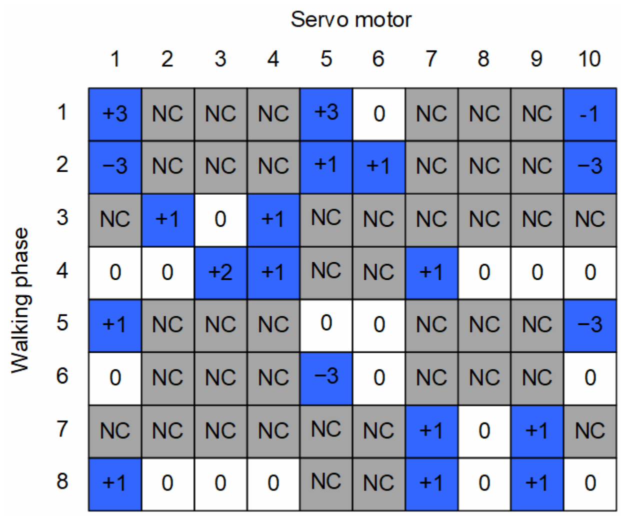

Walking phase \ Servo motor	1	2	3	4	5	6	7	8	9	10
1	+3	NC	NC	NC	+3	0	NC	NC	NC	-1
2	−3	NC	NC	NC	+1	+1	NC	NC	NC	−3
3	NC	+1	0	+1	NC	NC	NC	NC	NC	NC
4	0	0	+2	+1	NC	NC	+1	0	0	0
5	+1	NC	NC	NC	0	0	NC	NC	NC	−3
6	0	NC	NC	NC	−3	0	NC	NC	NC	0
7	NC	NC	NC	NC	NC	NC	+1	0	+1	NC
8	+1	0	0	0	NC	NC	+1	0	+1	0

Figure 18. The difference of gene values between the worst individual (the 4th) and the first individual

4. DISCUSSION AND CONCLUSION

The GA has been applied to optimize the quasi-dynamic walking of a 10-DoF humanoid robot. The robot represents a human's lower half-body, consisting of two feet, two legs, two thighs, and one waist. The joints include two ankles, two knees, and two hips. A novel fitness function is devised in order to achieve the purpose of increasing the walking performance of the robot in terms of high forward displacement and low deviation. The stability of the robot, in how it moves without falling down, is also taken into account.

The first individual is obtained by forward kinematics, from visualizing the required coordination between all the joints to make forward step movements of the robot. The remaining members of the initial population were derived from the first individual. Due to the durability issue of the humanoid robot, only four cycles of GA were conducted. In each cycle, up to 2 offspring are generated. Only the fittest 6 individuals survive into the next cycle. After the final cycle, the best fitness score of the population improves from 12.02 to 25.42, corresponding to an increase of 111.48 %. The walking distance is increased by 26.12 % from 25.33 to 31.94, while the deviation angle is reduced by 57.65 % from 25.39° to 10.75°.

Further possible studies include the development of a full-body humanoid robot with a certain task at hand. Optimizing the robot in a certain given direction, not only a straightforward direction, both with and without additional sensors, will also be a challenge that can be elaborated further.

REFERENCES

Afrisal, H., Munadi, M., Faris, M., and Ardi Sumbodo, B., 2019. The Development of Autonomous Human Humanoid Soccer Robot. *TEKNIK*, **40(1)**, 1-10.

Allgeuer, P., and Behnke, S., 2018, Bipedal Walking with Corrective Actions in the Tilt Phase Space. *IEEE-RAS 18th International Conference on Humanoid Robots (Humanoids)*, Beijing, China, 1-9.

Asif, M., Sabeel, M., Rahman, M., and Khan, Z.H., 2015, Waiter Robot – Solution to Restaurant Automation. *Proceedings of Multi-Disciplinary Student Research Conference*, Wah, Pakistan, 14-15.

Behnke, S., 2008, Humanoid Robots - From Fiction to Reality?. *KI-Zeitschrift*, 5-9.

Chande, P.S.V., and Sinha, D.M., 2008, Genetic Algorithm: A Versatile Optimization Tool. *International Journal of Information Technology*, **1(1)**, 7-13.

Bojan-Dragos, C.-A., Precup, R.-E., Preitl, S., Roman, R.-C., Hedrea, E.-L., and Szedlak-Stinean, A.-I., 2021, GWO-based Optimal Tuning of Type-1 and Type-2 Fuzzy Controllers for Electromagnetic Actuated Clutch Systems. *IFAC-PapersOnLine*, **54(4)**, 189-194.

Garcia, E., Jimenez, M.A., Santos, P.G.D., and Armada, M., 2007, The Evolution of Robotics Research. *IEEE Robotics & Automation Magazine*, **14(1)**, 90-103.

Haldurai, L., Madhubala, T., and Rajalakshmi, R., 2016, A Study on Genetic Algorithm and its Applications. *International Journal of Computer Sciences and Engineering*, **4(10)**, 139-143.

Hashimoto, K., and Takanashi, A., 2015, Biped Robot Research at Waseda University. *Journal of Robotics, Networking and Artificial Life*, **1(4)**, 261-264.

He, B., Si, Y., Wang, Z., and Zhou, Y., 2019, Hybrid CPG–FRI Dynamic Walking Algorithm Balancing Agility and Stability Control of Biped Robot. *Autonomous Robots*, **43(7)**, 1855-1856.

Hoffman, E.M., Caron, S., Ferro, F., Sentis, L., and Tsagarakis, N.G., 2019, Developing Humanoid Robots for Applications in Real-World Scenarios [From the Guest Editors]. *IEEE Robotics Automation Magazine*, **26(4)**, 17-19.

Hwang, K., Lin, L., and Yeh, K., 2015, Learning to Adjust and Refine Gait Patterns for a Biped Robot. *IEEE Transactions on Systems, Man, and Cybernetics: Systems*, **45(12)**, 1481-1490.

Jebari, K., Madiafi, M., and Elmoujahid, A., 2013, Parent Selection Operators for Genetic Algorithms. *International Journal of Engineering Research & Technology*, **2(11)**, 1141-1145.

Khan, L.A., Naeem, J., Khan U., and Hussain, S. Z., 2008, PID Control of Biped Robot. *International Conference on Robotics, Control, and Manufacturing Technology*, Hangzhou, China, 156-160.

Kobey, J., Glisson, M., and Mistry, M., 2012, Playing Catch and Juggling with Humanoid Robot. *International Conference on Humanoid Robots*, Osaka, Japan, 875-881.

Liu, C., Ning, J., An, K., and Chen, Q., 2017, Active Balance of Humanoid Movement Based on Dynamic Task-prior System. *International Journal of Advanced Robotic Systems*, **14(3)**, 1-13.

Lumoindong, C. W. D., and Sitompul, E., 2021, A prototype of an IoT-based pet robot with customizable functions (CoFiBotV2). *International Journal of Mechanical Engineering and Robotics Research*, **10(9)**, 510-518.

Maiorino, A., and Muscolo, G.G., 2020, Biped Robots with Compliant Joints for Walking and Running Performance Growing. *Frontiers in Mechanical Engineering*, **6(11)**, 1-11.

Mallawaarachchi, V., 2017, Introduction to Genetic Algorithms — Including Example Code. *Towards Data Science*. Available: https://towardsdatascience.com/introduction-to-genetic-algorithms-including-example-code-e396e98d8bf3.

Manikas, T., Ashenayi, K., and Wainwright, R., 2007, Genetic Algorithms for Autonomous Robot Navigation. *IEEE Instrumentation & Measurement Magazine*, **10(6)**, 26-31.

Mousavi, F.S., Ghassemi, P., Kalhor, A., and Masouleh, M.T., 2017, Dynamic Balance of a NAO H25 Humanoid Robot Based on Model Predictive Control. *IEEE 4th International Conference on Knowledge-Based Engineering and Innovation*, Tehran, Iran, 156-164.

Oztop, E., Franklin, D.W., Chaminade, and T., Cheng, G., 2005, Human-Humanoid Interaction: Is a Humanoid Perceived as a Human? *International Journal of Humanoid Robotics*, **2(4)**, 537-559.

Pandey, H.M., 2016, Performance Evaluation of Selection Methods of Genetic Algorithm and Network Security Concerns. *Procedia Computer Science*, **78**, 13-18.

Preitl, Z., Precup, R.-E., Tar, J.K., and Takács, M., 2006, Use of Multi-Parametric Quadratic Programming in Fuzzy Control Systems. *Acta Polytechnica Hungarica*, **3(3)**, 29-43.

Riley, M., and Atkeson, C., 2002, Robot Catching: Towards Engaging Human-humanoid Interaction. *Robots*, **12(1)**, 119-128.

Riley, M., Ude, A., and Atkeson, C.G., 2000, Methods for Motion Generation and Interaction with a Humanoid Robot: Case Studies of Dancing and Catching. *Proceeding AAAI and CMU Workshop on Interactive Robotics and Entertainment*, Pittsburgh, USA, 35-42.

Sandini, G., Sciutti, A., and Rea, F., 2019, Movement-Based Communication for Humanoid-Human Interaction. *Humanoid Robotics: A Reference, Springer*, 2169-2197.

Sastry, K., and Goldberg, D.E., 2002, Analysis of Mixing in Genetic Algorithms: A Survey. IlliGAL report no. 2002012, 1-15.

Šegota, S.B., Anđelić, N., Lorencin, I., Saga, M., and Car, Z., 2020, Path Planning Optimization of Six-Degree-of-Freedom Robotic Manipulators Using Evolutionary Algorithms. *International Journal of Advanced Robotic Systems*, **17(2)**, 1-16.

Sitompul, E., and Bukhori, I., 2014, A New Approach in Self-Generation of Fuzzy Logic Controller by Means of Genetic Algorithm. *6th International Conference on Information Technology and Electrical Engineering*, Yogyakarta, Indonesia, 394-399.

Sitompul, E., and Bunawan, A., 2011, Control of Traffic Light Using Fuzzy Logic and Harmony Search Algorithm. *3rd International Conference on Machine Learning and Computing*, Singapore, 112-116.

Soon, G.K., Guan, T.T., On, C.K., Alfred, R., and Anthony, P., 2013, A Comparison on the Performance of Crossover Techniques in Video Game. *IEEE International Conference on Control Systems, Computing and Engineering*, Penang, Malaysia, 493-498.

Zapata, H., Perozo, N., Angulo, W., and Contreras, J., 2020, A Hybrid Swarm Algorithm for Collective Construction of 3D Structures. *International Journal of Artificial Intelligence*, **18(1)**, 1-18.